

Received September 9, 2019, accepted October 10, 2019, date of publication October 25, 2019, date of current version November 5, 2019.

Digital Object Identifier 10.1109/ACCESS.2019.2948973

# Voltage Regulation and Power Management for Wireless Flow Sensor Node Self-Powered by Energy Harvester With Enhanced Reliability

YUSHEN HU<sup>1,2,3</sup>, ANXIN LUO<sup>1,3,4,5</sup>, JUNLEI WANG<sup>6</sup>,  
AND FEI WANG<sup>1,3,7</sup>, (Senior Member, IEEE)

<sup>1</sup>School of Microelectronics, Southern University of Science and Technology, Shenzhen 518055, China

<sup>2</sup>Department of Electronic and Computer Engineering, The Hong Kong University of Science and Technology

<sup>3</sup>Shenzhen Key Laboratory of 3rd Generation Semiconductor Devices, Shenzhen 518055, China

<sup>4</sup>State Key Laboratory of Analog and Mixed-Signal VLSI, Institute of Microelectronics, University of Macau (UM), Macau 999078, China

<sup>5</sup>Faculty of Science and Technology, University of Macau (UM), Macau 999078, China

<sup>6</sup>Engineering Research Center of Energy Saving Technology and Equipment of Thermal Energy System, Ministry of Education, Zhengzhou University, Zhengzhou 450000, China

<sup>7</sup>State Key Lab of Transducer Technology, Shanghai Institute of Microsystem and Information Technology, Chinese Academy of Sciences, Shanghai 200050, China

Corresponding author: Fei Wang (wangf@sustech.edu.cn)

This work was supported in part by the Shenzhen Science and Technology Innovation Committee under Grant JCYJ20170412154426330, in part by the Guangdong Natural Science Funds under Grant 2016A030306042 and Grant2018A050506001, and in part by the Materials Characterization and Preparation Center, Southern University of Science and Technology.

**ABSTRACT** This paper reports a voltage regulation method with power management to enhance the reliability and stability of the self-powered flow rate sensor. Triboelectric energy harvesters are used both as the sensing signals and the power supply. One channel of the raw voltage from wind flow is regulated to a stable signal by the integral circuit, while the other channel is used for energy harvesting to provide the power for the whole circuit. Power management chip with ultra-low power consumption has been utilized with micro controller unit and antenna for wireless transmission. A low deviation of less than 2.5% has been achieved for the flow sensing signal and the temperature has also been monitored simultaneously, which shows promising application for the central air-conditioning system in smart buildings.

**INDEX TERMS** Flow sensor, energy harvester, voltage regulation, wireless sensor networks (WSN).


## I. INTRODUCTION

Wireless sensor networks (WSN) have attracted more and more attentions for wide applications in the fields of industry, healthcare, and environmental monitoring, etc. Recently, another concept of “Internet of Things (IoT)” has also been developed, which typically consists of WSN, cameras, smartphones, and RFIDs, to collect data and track information for smart city [1], smart home [2], intelligent buildings [3], and industrial Internet of Things (IIoT) [4], [5]. However, the service life of WSN and IoT are limited by traditional batteries with finite capacity. Hence, they need other technology to solve this problem and prolong the life of themselves.

Energy harvesting (EH) technology has been developed in the past decade, as it can extract energy from ambient

environment to replace the batteries [6], [7]. Vibration based energy harvesters can be typically achieved by four principles, piezoelectricity [8]–[13], electromagnet [14]–[16], electrostatic [17]–[20] and triboelectricity methods. Piezoelectric EH utilizes the deformation of piezoelectric film to generate power. Faraday’s law of electromagnetic induction is the basic principle of electromagnet EH. Electrostatic EH output alternate voltage by changing the overlapping area or gap distance of capacitors with electret material, which can store the charge for a long period of time.

Recently, increasing research efforts have been made in water flow and wind flow EH field, because wind and tidal energy are important clean energy resources in the environment. For instance, Shan *et al.* [21] presented a double piezoelectric energy harvesters (DPEH) system to scavenge energy underwater. Wind flow [22], [23] energy has also been harvested using either electret materials [24] or triboelectric

The associate editor coordinating the review of this manuscript and approving it for publication was Resul Das .

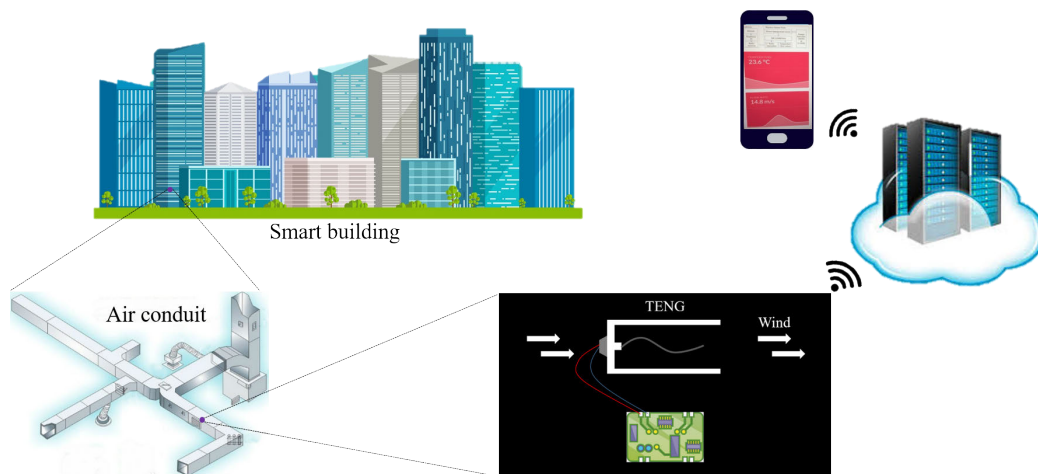


**FIGURE 1.** Wireless flow sensor node self-powered by energy harvester with application for air conditioning system in smart building.

nanogenerators (TENG) [25]–[28], to provide sustainable power supply for wireless sensors.

However, in the process of large-scale application of energy harvesting devices, the problem of energy and task assignment plagued the system. It is better for the WSN center to know the environment energy intensity of each node in order to assign more tasks to nodes with high environmental energy intensity, vice versa. Taking TENG device as an example, for TENG whose working environment is designed in central air conditioning pipeline, the collection of wind speed intensity is of great significance to the whole WSN system. A typical flow rate for the air pollution control system is less than  $15 \text{ m} \cdot \text{s}^{-1}$  while this value for the central air-conditioning system could be up to  $17.5 \text{ m} \cdot \text{s}^{-1}$  [29].

Conventional air flow sensors utilized the thermosensitive effect [30] or thermoelectric effect [31], where the measurement accuracy would be influenced by the variation of temperature. Furthermore, most of these sensors are powered by conventional batteries. The regular maintenance is difficult for the nodes in the air duct and blast pipe, which limits the scale of WSN.

On the other hand, self-powered sensors have been developed recently based on TENG for pressure sensing [32] and wind flow rate sensing [33], [34], where the generated voltage or current is dependent on the air flow. As illustrated in Fig. 1, a wireless flow sensor node self-powered by energy harvester can be mounted in the pipeline, which could monitor the temperature and flow rate of the central air conditioning system. The output voltage of the TENG, however, is generally irregular in large fluctuation range. Therefore, it is necessary to improve the measurement accuracy and reliability of the flow sensor for practical applications.

In this paper, we have developed a voltage regulation method to achieve stable sensing signal with low fluctuation for a wireless flow sensor node. We have demonstrated that the self-powered sensor nodes could regularly send out reliable flow rate wireless signal with deviation

lower than 2.5%, which is independent on the variation of temperature.

Compared with the previous article with the idea of using TENG as flow rate sensor [33], [34], this method can achieve much higher signal acquisition accuracy. To the best of our knowledge, the voltage regulation method has never been applied for self-powered sensing field yet. More importantly, voltage regulation method is potential to be applied to other types of energy harvester devices, where the output is typically related to the density and variation of the energy source.

This paper is organized as below: section II describes the system and device description, the principle of TENG device and voltage regulation method; section III gives the experimental setup in details; In section IV, we have shown the experimental results with discussion; And finally, a brief conclusion is given in section V.

## II. SYSTEM AND DEVICE DESIGN

As shown in Fig. 2, the self-powered wireless flow sensing node consists of energy harvesters (TENG), integral circuit for voltage regulation, power management, flow rate detection, micro controller unit (MCU), wireless signal transmission components, etc. Fig. 2(a) shows the two channels for energy and sensing signal outputs from the TENG. Fig. 2(b) includes the power management circuit, energy storage capacitor and flow rate detection circuit. When the capacitor has stored sufficient energy to drive the MCU, the control unit will generate a trigger signal to transmit the sensing information to the gateway through the antenna. A detailed flow chart of the system is shown in Fig. 3 and described below.

### A. SELF-POWERED WIRELESS FLOW RATE SENSING NODE

As shown in Fig.2 (a), we have used a TENG device both for energy harvesting and flow rate sensing. The TENG device consists of a flexible PTFE film, which contacts periodically with top and bottom metal electrodes when driven by the

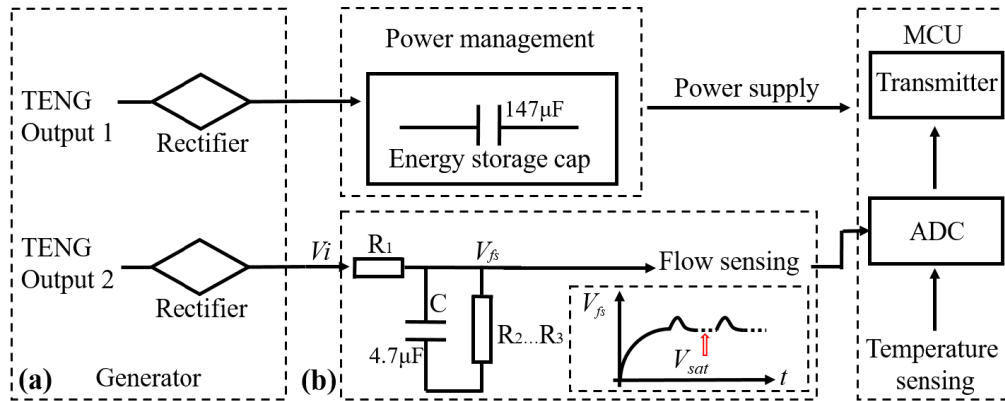


**FIGURE 2.** System diagram of self-powered wireless sensor node for both temperature and air flow detection. (a) Power source from triboelectric nanogenerator (TENG); (b) Signal transmitter part including components of power management, flow sensing with voltage regulation, and MCU with an ADC and a wireless transmitter.

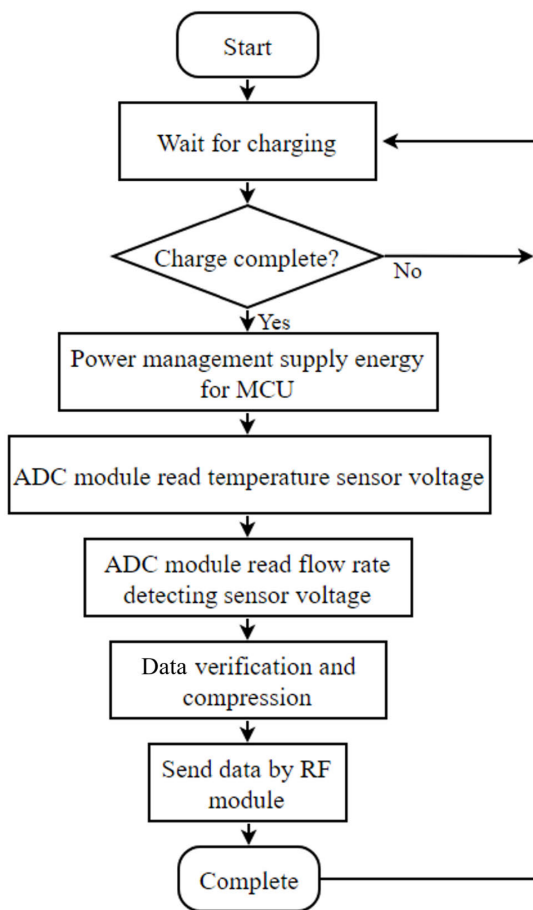


**FIGURE 3.** Flow chart of self-powered wireless temperature and flow rate sensor node.

air flow. Through a few rectifiers (DB107), the output power of the TENG is accumulated in a storage capacitor of  $147\ \mu\text{F}$  in a power management circuit. Meanwhile, one channel of the TENG output can simultaneously charge another capacitor of  $4.7\ \mu\text{F}$  for flow sensing shown in Fig.2 (b).

Flow chart of self-powered wireless temperature and flow rate sensor node has been presented in Fig.3. When the

storage capacitor is charged to a threshold voltage, the power management circuit will allocate certain amount of energy to a micro controller unit (MCU). The MCU drives ADC module to read the temperature and flow rate voltage, then convert them to applicable digital data. Both voltage signals of the flow rate sensing and the temperature sensing (from an embedded sensor in MCU) are transferred through an Analog-to-Digital Converter (ADC). Afterwards, the data is verified, and correct data will be compressed and sent to the receiver through the RF module. After completing this series of operations, the WSN re-entered the charging phase and repeat the cycle mentioned above.

In this work, a temperature sensor integrated in the MCU chip was used to demonstrate that the circuit and TENG can provide efficient power supply to drive two or more sensors at the same time.

### B. TENG DEVICE

Triboelectric nanogenerator is the core component of this wireless sensor node for power supply and flow sensing. Recently, there is an increasing research interest in TENG due to its simple flapping foil structure, and low manufacturing cost [35]. More importantly, the high efficiency of the TENG at low frequency is attractive for small-scale application, comparing with other air-flow energy harvesting devices such as traditional wind mills or wind turbines.

Triboelectricity could be generated when two different materials are forced to contact with each other. Based on this principle, triboelectric nanogenerator have been developed to transform mechanical energy into electric power for energy harvesting [22]–[25]. As shown in Figs. S1 and S2, a soft film of PTFE driven by wind periodically contacts a metal layer and changes the surface potential of both materials. The overall size of the TENG we used in this experiment is  $67\ \text{mm} \times 22\ \text{mm} \times 10\ \text{mm}$ . Detailed information about the TENG can be found in our previous work [25].

Fig. S1 presents the image of a TENG device with double contact-pairs of electret and electrode. Therefore, there are two output channels in Fig.2. Output 1 with higher output

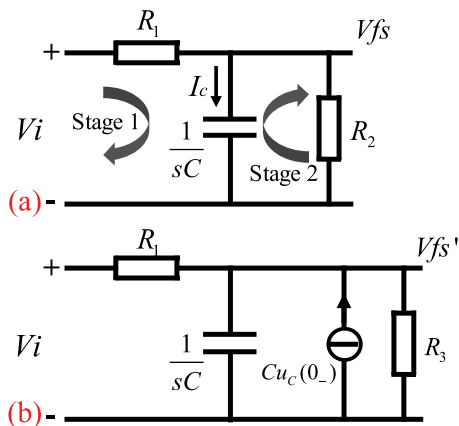


FIGURE 4. The core circuit model at (a) stable stage, and (b) signal reading stage.

power was used as energy harvesting; meanwhile, the other output 2 works as the signal for flow sensing. The TENG device is mounted on a slider rail with an air blower at one end. Prior to the test, we have characterized the system at various wind speeds by changing the position of the device on the rail.

C. VOLTAGE REGULATION METHOD

Unlike the traditional TENG sensors where the raw voltage signal was directly used [32], we have developed a new flow rate sensing circuit with a voltage regulation method. As shown in Fig.2(b), dynamic balance could be achieved between the energy harvested from the TENG and the energy dissipation from the sensing circuit. After a short warm-up process, a saturation voltage  $V_{sat}$  with low deviation could be detected, which exhibits a reliable relationship with the air flow rate.

The voltage regulation circuit is shown in Fig.4(a), which could be described by a system function:

$$H(s) = \frac{1}{1 + \frac{R_1}{R_2} + sCR_1} \tag{1}$$

where  $C$  is the capacitance of the flow sensing capacitor,  $R_1$  and  $R_2$  are the effective resistance of TENG device and flow sensor circuit, respectively. The system function in time domain can be derived from equation (1) as:

$$f(t) = \frac{1}{R_1 C} e^{-t(R_1+R_2)/(CR_1R_2)} \tag{2}$$

After the  $V_i$  signal was input to this system, the output voltage value  $V_{fs}$  would eventually saturate to a certain level. When the ADC starts sampling, the equivalent resistance  $R_2$  changed to  $R_3$ , and the circuit at this time can be represented by Fig.4 (b).

Based on the simplified model shown in Fig.4 (a), the raw open voltage data in Fig.5 (a) is applied to the simulation circuit model and theoretical model, then the flow sensing voltage could either be simulated from an LT-Spice software or be calculated from the theoretical analysis based on

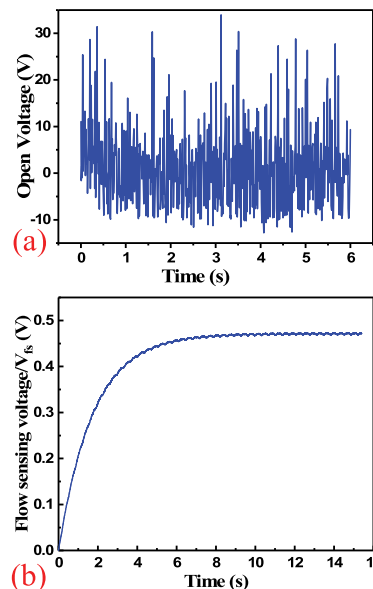


FIGURE 5. (a) raw input voltage and (b)simulation result.

Equation (3), which is the convolution of input raw open voltage and system function in time domain.

$$V_{fs}(t) = V_i(t) \otimes \frac{1}{R_1 C} e^{-t(R_1+R_2)/(CR_1R_2)} \tag{3}$$

The simulation results based on equation 3 are shown in Fig.5(b). After several seconds, it reaches a stable state,  $V_{fs}$  can be read at this state, which is about 0.45 V. Equation 3 derived from S-domain is suitable for simulation. In addition, time domain model could also be made with Equation (4), which properly represents the nature of the integration circuit:

$$V_{fs}(t) = e^{-\frac{t}{R_2 C}} \times \frac{1}{C} \times \left[ \int_0^t \frac{V_i(t)}{R_1} e^{\frac{t}{R_2 C}} dt + const \right] \tag{4}$$

where  $C$ ,  $R_1$  and  $R_2$  have been defined in the Equation (1).  $V_i(t)$  is the raw voltage generated from TENG, and  $const$  defines the initial condition.

It should be noted that the time for stabilization process is dependent on the time constant, which can be tuned by the  $C_1$  and  $R_2$  for rapid response.

III. EXPERIMENTAL SETUP

Fig.6 illustrates the sensor node with components for the wireless transmitter part and the receiver part. All the transmitter components including the power management, the flow sensing, and the MCU are powered by TENG. The receiver MCU is connected with a raspberry Pi to decode and upload the sensing signals.

The TENG device was mounted on a slider that is positioned a certain distance from the blower, it supplies power to the energy management circuit driven by the wind. the power management module waits for charging until the voltage across the storage capacitor reaches the threshold voltage of 4.03 V. When the threshold voltage is achieved, the storage

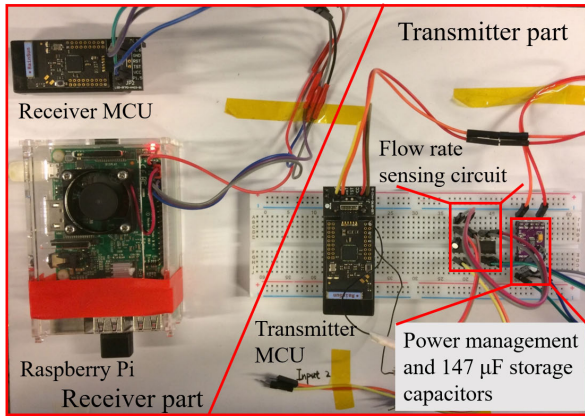


**FIGURE 6.** Wireless sensor node with power management circuit, storage capacitor, flow rate sensing circuit and transmitter MCU are shown on the right, server (raspberry pi) plus a receiver are shown on the left.

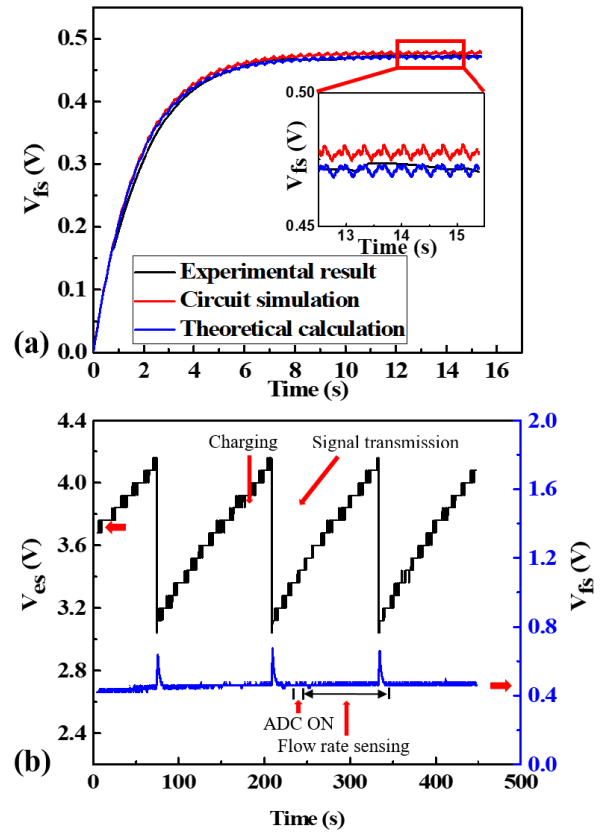
capacitor will release energy to the MCU and the temperature sensor (flow rate sensor was charged by one channel of TENG device). Within 35ms of the MCU’s operation, MCU drives the ADC module to read the temperature and flow rate voltage and send them to server.

To reduce the power consumption of the system, we have used a power management chip with ultra-low power consumption LTC-3588 (Extremely low quiescent current, 450nA typical). Fig. S3 shows the circuits of the power management component and the MCU. We have also used an integrated temperature sensor (embedded in CC430F5137), whose detailed information on can be found in the datasheet [36]. An antenna with the lowest transmission power of  $-30$  dBm has also been used in the system.

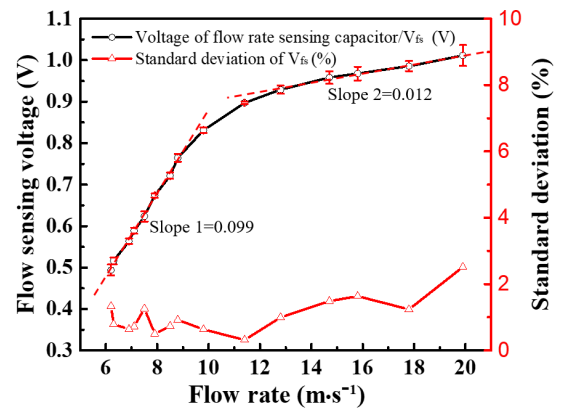
#### IV. WIRELESS SENSING PERFORMANCE

Fig.7 presents the voltage of the flow sensing capacitor ( $V_{fs}$ ) and the energy storage capacitor during the measurement ( $V_{es}$ ). When the wild voltage from TENG is applied to the voltage regulation circuit,  $V_{fs}$  will saturate at a stable voltage with fluctuation of less than 1%. During that, a warm-up process of 10 s is necessary, which provides a reliable signal for flow rate sensing. From Fig.7 (a), the measured voltage of flow sensing agrees well with the simulation and the theoretical calculation. It should be noted that the effective resistance of the circuit could change due to ADC process and wireless signal transmission. Therefore, a transient turbulence of  $V_{fs}$  can be observed during the test, as shown in Fig.7 (b). At a flow rate of  $6.2 \text{ m} \cdot \text{s}^{-1}$ , it takes about 135 s to charge the storage capacitor from 3.12 V to 4.03 V, which is set as the threshold voltage for wireless signal transmission. Therefore, the overall storage energy is calculated as  $472.5 \mu\text{J}$  for each cycle of 135 s, and the average storage power is about  $3.5 \mu\text{W}$  at the flow rate of  $6.2 \text{ m} \cdot \text{s}^{-1}$ . It should be noted that, this charging time can be easily tuned by the storage capacitance and the threshold voltage, which means the duty cycles can be improved as well.

The relationship between the flow rate of wind and the flow sensing voltage is shown in Fig.8. As described in [10],



**FIGURE 7.** (a) Voltage of flow rate sensing capacitor from experiment, comparing with the LT-Spice simulation and theoretical calculation; (b) Voltages of the energy storage capacitor (top curve) and flow sensing capacitor (bottom curve) during the test.



**FIGURE 8.** The saturated voltage of flow sensing  $V_{sat}$  (top curve) and the standard deviation of  $V_{sat}$  (bottom curve).

an air blower is used to generate the wind with flow rate ranging from  $6.2 \text{ m} \cdot \text{s}^{-1}$  to  $19.9 \text{ m} \cdot \text{s}^{-1}$ , and a commercial anemometer is used to monitor the flow rate during the measurement. When the flow rate increases from  $6.2 \text{ m} \cdot \text{s}^{-1}$  to  $9.8 \text{ m} \cdot \text{s}^{-1}$ ,  $V_{sat}$  increases remarkably from 0.49 V to 0.83 V, and an approximately linear relationship has been obtained with slope  $0.099 \text{ V} \cdot \text{s} \cdot \text{m}^{-1}$ . For flow rate higher than  $9.8 \text{ m} \cdot \text{s}^{-1}$ ,  $V_{sat}$  keeps increasing according to the increased air flow up to  $19.9 \text{ m} \cdot \text{s}^{-1}$  with a gentler slope  $0.012 \text{ V} \cdot \text{s} \cdot \text{m}^{-1}$ , which is mainly due to the output saturation of TENG.

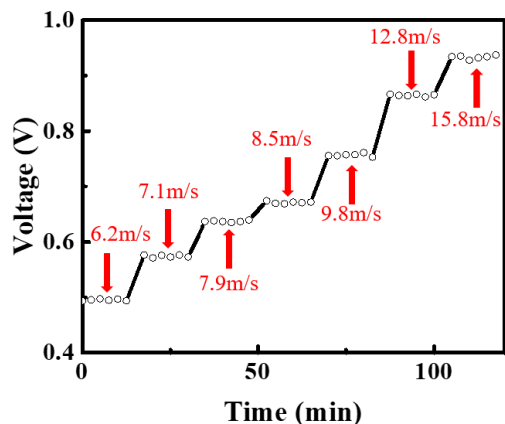


**FIGURE 9.** The stable sensing voltage of 6 measurements performed at each flow rate. The time span between two adjacent points is about 150s.

More importantly, we have tested more than 6 times at each flow rate to interrogate the reliability of flow rate sensing measurement. Fig.9 shows the detailed measurements when the air flow rate increases from  $6.2 \text{ m} \cdot \text{s}^{-1}$  to  $15.8 \text{ m} \cdot \text{s}^{-1}$  step by step. The sensor can clearly tell the difference of the flow rate and provides stable and repeatable sensing voltage for the 6 measured points at each step. Compared with the large deviation from the raw voltage signals, the reliability of our flow rate sensor has been greatly enhanced by the voltage regulation method. For instance, the variation of the flow sensing signal in [33] demonstrates a deviation higher than 10% for the sensing current. In another report [34], the deviations of the measured output voltage and current were higher than 50% for the flow rate ranging from  $6 \text{ m} \cdot \text{s}^{-1}$  to  $14 \text{ m} \cdot \text{s}^{-1}$ . In this work, the maximum standard deviation of  $V_{\text{sat}}$  is only 2.5% at the full measurement range.

Together with a temperature sensor embedded in the MCU, the flow rate sensor has been used for a self-powered wireless sensor node to monitor environment temperature and air flow simultaneously. The measurement setup is shown in Fig. S4, and a supplementary video is also recorded during the test. A 2.6-hours experiment was used to demonstrate the reliability and practicability. The detailed results of temperature and air flow sensing are shown in Fig.10. During the 2.6 hours test, the self-powered sensor node can send wireless signals every 140 s with the information of both temperature and air flow rate in Fig. 10(a). The sensor node has also detected the temperature change when it is moved from a warm spot to a cool place while the measured flow rate is kept consistent, which proves that the flow sensing is independent on the temperature variation. We developed a website to display the temperature and flow rate data, users can get the data by using a mobile phone conveniently in Fig.10 (b).

In order to illustrate that the energy of the WSN is sufficient to drive two or more different types of sensors, we calculate the power consumption of the device. The voltage regulation approach only requires a few milliseconds for setup, including data sampling and transmitting. As demonstrated in Fig.7 (b), once the energy stored in the capacitor reaches

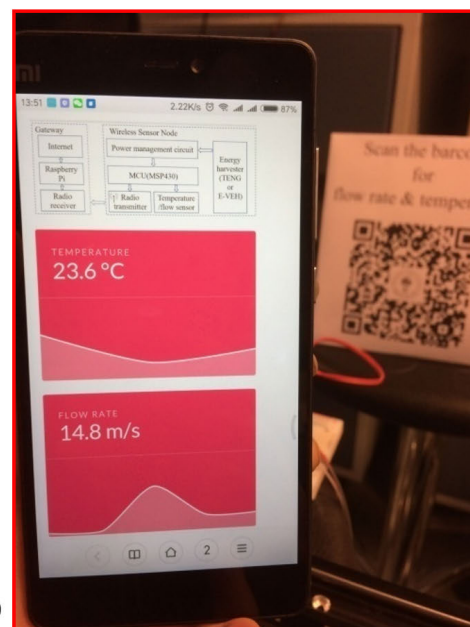
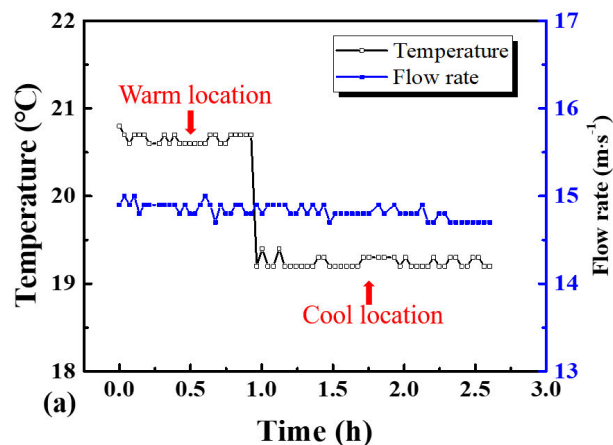


**FIGURE 10.** (a) A wireless sensing test for both the temperature and air flow rate in environment monitoring for 2.6 hours. The self-powered sensor node can acquire the sensing signals once per 140 seconds at an air flow of  $14.7 \text{ m} \cdot \text{s}^{-1}$ ; (b) application in mobile phone.

the threshold then start to discharge, it only takes about 35 ms to read and send one set of temperature and flow rate data.

In this method, the energy management chip will supply power to the MCU when the voltage across the storage capacitor reaches 4.03 V. The MSP430 reads the data of the chip's internal temperature sensor and the voltage across flow rate detect capacitor by ADC channel 2. After the modulation, the signal is transmitted through the antenna.

The power consumption of MCU in V-max method can be calculated by Equation 4 with the experimental data:

$$P = \frac{E}{t} = \frac{\frac{1}{2} \times C \times V_{init}^2 - \frac{1}{2} \times C \times V_{final}^2}{t} = 13.66mW \tag{5}$$

The operating power of this wireless sensor node is 13.66 mW, and the power consumption is mainly allocated to the ADC sampling and wireless transmission parts. It should

be noted that the power consumption of antenna is 10 dBm to transmit the signal to a remote gateway (>0.7 km) in a complex work environment. Temperature and flow rate data are compressed into 2 bytes, which causes the fluctuations in the data we saw on the web page to be more pronounced in Fig. 10(a). In fact, by increasing the capacitance of the energy storage capacitor, the node will be able to transfer more data or carry more different types of sensors, although it will increase the charging time.

## V. CONCLUSION

In this paper, we have proposed a voltage regulation method with integral circuit and power management for self-powered wireless flow rate sensing. A regulated voltage signal has been used for the flow sensing instead of the raw voltage from TENG. The measured regulated voltage shows excellent agreement with the simulation model and the theoretical calculation. With the voltage regulation method, the reliability of the flow sensor node has been greatly enhanced. Compared to the previous work using the energy harvester to drive wireless sensor nodes, the design of the energy harvesting device as a sensor sensitive to the energy source will greatly improve the robustness and efficiency of the entire wireless sensor network. The voltage regulation method might be applied to other devices or self-powered systems with unstable signals. We will try to explore the application and study the compatibility and scalability in the future.

## REFERENCES

- [1] A. Zanella, N. Bui, A. Castellani, L. Vangelista, and M. Zorzi, "Internet of Things for smart cities," *IEEE Internet Things J.*, vol. 1, no. 1, pp. 22–32, Feb. 2014.
- [2] B. L. R. Stojkoska and K. V. Trivodaliev, "A review of Internet of Things for smart home: Challenges and solutions," *J. Cleaner Prod.*, vol. 140, no. 3, pp. 1454–1464, 2017.
- [3] N. K. Suryadevara, S. C. Mukhopadhyay, S. D. T. Kelly, and S. P. S. Gill, "WSN-based smart sensors and actuator for power management in intelligent buildings," *IEEE/ASME Trans. Mechatronics*, vol. 20, no. 2, pp. 564–571, Apr. 2015.
- [4] C. Li, Y. Fu, Z. Liu, X.-Y. Liu, W. Wu, and L. Xiong, "Spectrum trading for energy-harvesting-enabled Internet of Things in harsh environments," *IEEE Access*, vol. 6, pp. 16712–16726, 2018.
- [5] L. Hou, S. Tan, Z. Zhang, and N. W. Bergmann, "Thermal energy harvesting WSNs node for temperature monitoring in IIoT," *IEEE Access*, vol. 6, pp. 35243–35249, 2018.
- [6] P. D. Mitcheson, E. M. Yeatman, G. K. Rao, A. S. Holmes, and T. C. Green, "Energy harvesting from human and machine motion for wireless electronic devices," *Proc. IEEE*, vol. 96, no. 9, pp. 1457–1486, Sep. 2008.
- [7] F. K. Shaikh and S. Zeadally, "Energy harvesting in wireless sensor networks: A comprehensive review," *Renew. Sustain. Energy Rev.*, vol. 55, pp. 1041–1054, Mar. 2016.
- [8] J. Jia, X. Shan, D. Upadrashta, T. Xie, Y. Yang, and R. Song, "Modeling and analysis of upright piezoelectric energy harvester under aerodynamic vortex-induced vibration," *Micromachines*, vol. 9, no. 12, p. 667, 2018.
- [9] Y. Wu, J. Qiu, S. Zhou, H. Ji, Y. Chen, and S. Li, "A piezoelectric spring pendulum oscillator used for multi-directional and ultra-low frequency vibration energy harvesting," *Appl. Energy*, vol. 231, pp. 600–614, Dec. 2018.
- [10] X. Mei, S. Zhou, Z. Yang, T. Kaizuka, and K. Nakano, "The benefits of an asymmetric tri-stable energy harvester in low-frequency rotational motion," *Appl. Phys. Express*, vol. 12, no. 5, 2019, Art. no. 057002.
- [11] S. Li, Z. Peng, A. Zhang, and F. Wang, "Dual resonant structure for energy harvesting from random vibration sources at low frequency," *AIP Adv.*, vol. 6, no. 1, 2016, Art. no. 015019.
- [12] S. Li, A. Crovetto, Z. Peng, A. Zhang, O. Hansen, M. Wang, X. Li, and F. Wang, "Bi-resonant structure with piezoelectric PVDF films for energy harvesting from random vibration sources at low frequency," *Sens. Actuators A, Phys.*, vol. 247, pp. 547–554, Aug. 2016.
- [13] F. Liu, Y. Zhang, O. Dahlsten, and F. Wang, "Intelligently chosen interventions have potential to outperform the diode bridge in power conditioning," *Sci. Rep.*, vol. 9, p. 8994, Jun. 2019.
- [14] Q. Zhang and E. S. Kim, "Vibration energy harvesting based on magnet and coil arrays for watt-level handheld power source," *Proc. IEEE*, vol. 102, no. 11, pp. 1747–1761, Nov. 2014.
- [15] K. Fan, S. Liu, H. Liu, Y. Zhu, W. Wang, and D. Zhang, "Scavenging energy from ultra-low frequency mechanical excitations through a bi-directional hybrid energy harvester," *Appl. Energy*, vol. 216, pp. 8–20, Apr. 2018.
- [16] K. Fan, M. Cai, F. Wang, L. Tang, J. Liang, Y. Wu, H. Qu, and Q. Tan, "A string-suspended and driven rotor for efficient ultra-low frequency mechanical energy harvesting," *Energy Convers. Manage.*, vol. 198, Oct. 2019, Art. no. 111820.
- [17] Y. Zhang, Y. Hu, X. Guo, and F. Wang, "Micro energy harvester with dual electrets on sandwich structure optimized by air damping control for wireless sensor network application," *IEEE Access*, vol. 6, pp. 26779–26788, 2018.
- [18] Y. Zhang, T. Wang, A. Luo, Y. Hu, X. Li, and F. Wang, "Micro electrostatic energy harvester with both broad bandwidth and high normalized power density," *Appl. Energy*, vol. 212, pp. 362–371, Feb. 2018.
- [19] Y. Zhang, T. Wang, A. Zhang, Z. Peng, D. Luo, R. Chen, and F. Wang, "Electrostatic energy harvesting device with dual resonant structure for wideband random vibration sources at low frequency," *Rev. Sci. Instrum.*, vol. 87, no. 12, 2016, Art. no. 125001.
- [20] Y. Suzuki, D. Miki, M. Edamoto, and M. Honzumi, "A MEMS electret generator with electrostatic levitation for vibration-driven energy-harvesting applications," *J. Micromech. Microeng.*, vol. 20, no. 10, 2010, Art. no. 104002.
- [21] X. Shan, H. Li, Y. Yang, J. Feng, Y. Wang, and T. Xie, "Enhancing the performance of an underwater piezoelectric energy harvester based on flow-induced vibration," *Energy*, vol. 172, pp. 134–140, Apr. 2019.
- [22] J. Wang, L. Tang, L. Zhao, and Z. Zhang, "Efficiency investigation on energy harvesting from airflows in HVAC system based on galloping of isosceles triangle sectioned bluff bodies," *Energy*, vol. 172, pp. 1066–1078, Apr. 2019.
- [23] G. Hu, J. Wang, Z. Su, G. Li, H. Peng, and K. C. S. Kwok, "Performance evaluation of twin piezoelectric wind energy harvesters under mutual interference," *Appl. Phys. Lett.*, vol. 115, no. 7, 2019, Art. no. 073901.
- [24] M. Perez, S. Boisseau, P. Gasnier, J. Willemin, and J. L. Reboud, "An electret-based aeroelastic flutter energy harvester," *Smart Mater. Struct.*, vol. 24, no. 3, Feb. 2015, Art. no. 035004.
- [25] Y. Wu, Y. Hu, Z. Huang, C. Lee, and F. Wang, "Electret-material enhanced triboelectric energy harvesting from air flow for self-powered wireless temperature sensor network," *Sens. Actuators A, Phys.*, vol. 271, pp. 364–372, Mar. 2018.
- [26] Z. Quan, C. B. Han, T. Jiang, and Z. L. Wang, "Robust thin films-based triboelectric nanogenerator arrays for harvesting bidirectional wind energy," *Adv. Energy Mater.*, vol. 6, no. 5, 2016, Art. no. 1501799.
- [27] X. Cheng, Z. Song, L. Miao, H. Guo, Z. Su, Y. Song, and H.-X. Zhang, "Wide range fabrication of wrinkle patterns for maximizing surface charge density of a triboelectric nanogenerator," *J. Microelectromech. Syst.*, vol. 27, no. 1, pp. 106–112, Feb. 2018.
- [28] T. Chen, Y. Xia, W. Liu, H. Liu, L. Sun, and C. Lee, "A hybrid flapping-blade wind energy harvester based on vortex shedding effect," *J. Microelectromech. Syst.*, vol. 25, no. 5, pp. 845–847, Oct. 2016.
- [29] S. K. Wang, *Handbook of Air Conditioning and Refrigeration*, vol. 49, 2000, p. 798.
- [30] W. Xu, K. Song, S. Ma, B. Gao, Y. Chiu, and Y.-K. Lee, "Theoretical and experimental investigations of thermoresistive micro calorimetric flow sensors fabricated by CMOS MEMS technology," *J. Microelectromech. Syst.*, vol. 25, no. 5, pp. 954–962, Oct. 2016.
- [31] R. Buchner, K. Froehner, C. Sosna, W. Benecke, and W. Lang, "Toward flexible thermoelectric flow sensors: A new technological approach," *J. Microelectromech. Syst.*, vol. 17, no. 5, pp. 1114–1119, Oct. 2008.
- [32] Q. Shi, H. Wang, T. Wang, and C. Lee, "Self-powered liquid triboelectric microfluidic sensor for pressure sensing and finger motion monitoring applications," *Nano Energy*, vol. 30, pp. 450–459, Dec. 2016.

[33] Y. Su, G. Xie, T. Xie, H. Zhang, Z. Ye, Q. Jing, H. Tai, X. Du, and Y. Jiang, "Wind energy harvesting and self-powered flow rate sensor enabled by contact electrification," *J. Phys. D, Appl. Phys.*, vol. 49, no. 21, Apr. 2016, Art. no. 215601.

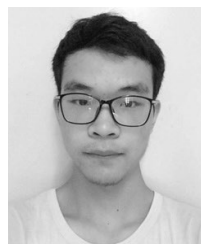
[34] Y. Yang, G. Zhu, H. Zhang, J. Chen, X. Zhong, Z.-H. Lin, Y. Su, P. Bai, X. Wen, and Z. L. Wang, "Triboelectric nanogenerator for harvesting wind energy and as self-powered wind vector sensor system," *ACS Nano*, vol. 7, no. 10, pp. 9461–9468, Sep. 2013.

[35] B. N. Chandrashekar, A. S. Smitha, Y. Wu, N. Cai, Y. Li, Z. Huang, W. Wang, R. Shi, J. Wang, S. Liu, S. Krishnaveni, F. Wang, and C. Cheng, "A universal stamping method of graphene transfer for conducting flexible and transparent polymers," *Sci. Rep.*, vol. 9, p. 3999, Mar. 2019.

[36] *CC430F613x, CC430F612x, CC430F513x MSP430 SoC With RF Core*. [Online]. Available: <http://www.ti.com.cn/cn/lit/ds/symlink/cc430f5137>



**JUNLEI WANG** received the B.S and Ph.D. degrees in power engineering from Chongqing University, Chongqing, in 2009 and 2014, respectively. Since 2019, he has been an Associate Professor with Zhengzhou University, China. His current research interests include energy harvesting from ambient environment, especially from flow-induced vibrations, e.g., vortex induced vibrations, galloping and wake-induced vibrations, interaction effect between the flow and mechanical vibrations, suppression of flow-induced vibrations, and application of nonlinear designs in flow-induced vibratory systems.



**YUSHEN HU** received the bachelor's degree from the Department of Electrical and Electronic Engineering, Southern University of Science and Technology, China, in 2018. He is currently pursuing the joint Ph.D. degree with the School of Microelectronics, Southern University of Science and Technology, and the Department of Electronic and Computer Engineering, The Hong Kong University of Science and Technology. His current research interests include circuit design and test for energy harvesters and self-powered wireless sensor network systems.



**ANXIN LUO** received the B.Eng. degree in micro-electronics and engineering from the Southern University of Science and Technology (SUSTech), Shenzhen, China, in 2017. He is currently pursuing the joint Ph.D. degree with the School of Microelectronics, SUSTech, and the Institute of Microelectronics, University of Macau (UM). His current research interests include energy harvester design and fabrication and power management circuit design for energy harvester.



**FEI WANG** (S'06–M'09–SM'12) received the B.S. degree in mechanical engineering from the University of Science and Technology of China, Hefei, China, in 2003, and the Ph.D. degree in microelectronics from the Shanghai Institute of Microsystem and Information Technology, Chinese Academy of Science, Shanghai, China, in 2008.

He was a Postdoctoral Researcher with the Department of Micro- and Nano-technology, Technical University of Denmark, where he has been an Assistant Professor, since 2010. Since 2013, he has also been an Associate Professor with the Southern University of Science and Technology, China. His current research interests include micro energy harvesting, MEMS and NEMS sensors, and semiconductor testing.

Dr. Wang served as a TPC Member for the 19th International Conference on Solid-State Sensors, Actuators and Microsystems (Transducers 2017), the 13th International Conference on Nano/Micro Engineered and Molecular Systems (NEMS 2018), and the International Conference on Manipulation, Manufacturing and Measurement on the Nanoscale (the IEEE 3M-NANO), from 2014 to 2017.

...